Chemical Science

ROYAL SOCIETY OF CHEMISTRY

EDGE ARTICLE

View Article Online
View Journal | View Issue

Check for updates

Cite this: *Chem. Sci.*, 2023, **14**, 4928

All publication charges for this article have been paid for by the Royal Society of Chemistry

Received 3rd January 2023
Accepted 13th March 2023

DOI: 10.1039/d3sc00042g

rsc.li/chemical-science

Open Access Article. Published on 19 April 2023. Downloaded on 2/11/2026 12:40:17 AM. This article is licensed under a Creative Commons Attribution-NonCommercial 3.0 Unported Licence.

Tantalum ureate complexes for photocatalytic hydroaminoalkylation†

Han Hao, ‡[a] Manfred Manßen ‡[b] and Laurel L. Schafer *[c]

Using a tantalum ureate pre-catalyst, photocatalytic hydroaminoalkylation of unactivated alkenes with unprotected amines at room temperature is demonstrated. The combination of $Ta(CH_2SiMe_3)_3Cl_2$ and a ureate ligand with a saturated cyclic backbone resulted in this unique reactivity. Preliminary investigations of the reaction mechanism suggest that both the thermal and photocatalytic hydroaminoalkylation reactions begin with N–H bond activation and subsequent metallaaziridine formation. However, a select tantalum ureate complex, through ligand to metal charge transfer (LMCT), results in photocatalyzed homolytic metal–carbon bond cleavage and subsequent addition to unactivated alkene to afford the desired carbon–carbon bond formation. Origins of ligand effects on promoting homolytic metal–carbon bond cleavage are explored computationally to support enhanced ligand design efforts.

Introduction

Advances in homogenous photoredox catalysis for amine and N-heterocycle alkylation have been extensively reported in recent years.[1–4] By using the energy of optimized light sources, many photoredox transformations can be achieved at ambient temperatures. This approach is ideal for reactions involving sensitive substrates as elevated temperatures are not required to overcome high-energy barriers. However, among the photocatalytic systems developed to facilitate α-alkylation of amines, most rely on classic noble metal photoredox catalysts such as $[Ru(bpy)_3]^{2+}$- or $[Ir(ppy)_3]$.[1–3,5–11] Alternatively, there has been recent attention on the use of earth abundant metal complexes in photocatalytic C–C bond formation in arylamine–arylamine dehydrogenative coupling,[12,13] but examples using alkylamine substrates are rare.[14–16]

Early transition metal catalyzed hydroaminoalkylation is a reaction for the formation of a new C_{sp^3}–C_{sp^3} bond by hydrofunctionalization of C=C multiple bonds with a C–H bond α- to an amine.[17–21] It is completely atom-economic and avoids pre-functionalized coupling partners in that simple secondary amines and alkenes can be used directly. Also, less toxic and less expensive early transition metals from groups 3, 4 and 5, including earth abundant metals like titanium can be used as catalysts.[22–26] In recent years this strategy has proven to be an efficient, thermally promoted reaction. However, like many other C–H functionalization reactions, this transformation often requires very high reaction temperatures, even up to 180 °C.[27–31] Even though a variety of early transition metal complexes for hydroaminoalkylation have been reported, room temperature reactivity is rare. To date there is one Ta phosphoramidate complex that can promote reactivity with styrenes and unprotected dialkyl secondary amines at ambient temperature,[32] and more recently the Doye group, inspired by earlier work of Hou on scandium-catalyzed hydroaminoalkylation,[33,34] reported a cationic titanium-catalyst for hydroaminoalkylation of alkenes with tertiary amines at room temperature.[35]

An alternative low-temperature activation strategy takes advantage of photoredox catalysis for hydroaminoalkylation. Amines undergo single electron oxidation chemistry,[36,37] to form α-aminoalkyl radical intermediates that can react further with alkenes. To date, several systems based on late transition metal (LTM) photoredox catalysts have been developed for hydroaminoalkylation. For example, in 2012, the Nishibayashi group first reported hydroaminoalkylation of electron deficient, activated alkenes with tertiary amines *via* α-aminoalkyl radicals formed by a classic iridium photocatalyst (Scheme 1a).[38] Xu and Li demonstrated that the addition of α-aminoalkyl radicals to activated acrylate derivatives could be achieved with $[Ru(bpy)_3][BF_4]_2$ as a photoredox catalyst.[39] The Rovis group showed that dual metal catalysis, using an Ir photocatalyst in combination with a cobalt complex, can be used for the mild hydroaminoalkylation of dienes with tertiary amines (Scheme 1b).[40] Furthermore, they demonstrated that this strategy could be extended to the direct alkylation of primary amines by "protection" of the amine with CO_2 to form a carbamate

[a]*Department of Chemistry, University of Toronto, Toronto, Ontario M5S 3H6, Canada*
[b]*Institut für Anorganische Chemie, Eberhard Karls Universität Tübingen, Auf der Morgenstelle 18, 72076, Tübingen, Germany*
[c]*Department of Chemistry, University of British Columbia, Vancouver, British Columbia V6T 1Z4, Canada. E-mail: schafer@chem.ubc.ca*

† Electronic supplementary information (ESI) available. See DOI: https://doi.org/10.1039/d3sc00042g

‡ These authors contributed equally to this work.

© 2023 The Author(s). Published by the Royal Society of Chemistry

Open Access Article. Published on 19 April 2023. Downloaded on 2/11/2026 12:40:17 AM. This article is licensed under a Creative Commons Attribution-NonCommercial 3.0 Unported Licence.

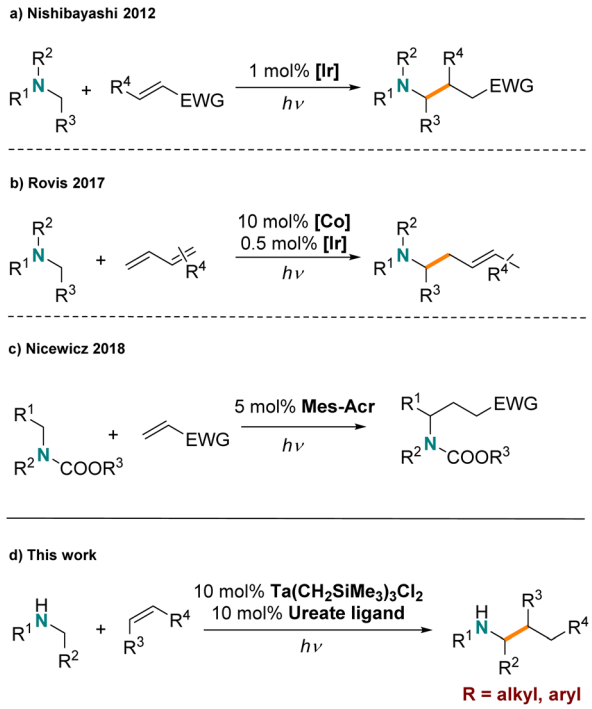

Scheme 1 Examples for photocatalyzed hydroaminoalkylations

functionality *in situ*.[41] Moreover, organic photosensitizers have been reported to facilitate similar chemistry by the Nicewicz group (Scheme 1c), showing the promising potential of organo-photocatalysis.[42]

However established LTM and organic photocatalysts are not effective for the regioselective hydroaminoalkylation of unactivated alkenes. Typically photoredox hydroaminoalkylation reactions are limited to activated alkenes and amines. For example α,β-unsaturated alkenes are used as substrate, which can efficiently harvest amine radicals generated by photoactivation.[38,39,42–45] Additionally, primary and secondary amines are easily over-oxidized and are not well tolerated without protection. Recently, the Cresswell group successfully overcame this challenge by using a hydrogen-atom-transfer (HAT) reagent together with organic photocatalysts to achieve styrene hydroaminoalkylation with unprotected primary alkylamines.[46]

Thermally promoted early-transition-metal catalyzed hydroaminoalkylation is efficient with unactivated alkenes and unprotected amines, but high temperatures are usually required. Meanwhile, early-transition-metal complexes featuring M–C_{sp^3} bonds are known to undergo light induced homolytic cleavage.[47–50] For example, the Ta(v)–Ta(iv) single-electron redox couple is readily accessible through such light induced processes.[51] We questioned if these reactivity trends could be harnessed to realize inexpensive and abundant early-transition-metal complexes for photocatalytic hydroaminoalkylation of unactivated alkenes under mild conditions. To date the handful of reported early-transition-metal photocatalysts are limited to dehalogenative reduction/homocoupling and olefin reduction reactions;[52–55] amine functionalization chemistry has not yet been disclosed. Herein, we report the first example of early-transition-metal photocatalytic hydroamino-alkylation using an organometallic tantalum ureate complex (Scheme 1d). This reaction features the use of unprotected amines and affords an alternative mechanism for achieving photocatalytic hydroaminoalkylation to include unactivated alkenes.

Result and discussion

Early transition metal complex reactivity screening

Simple homoleptic $Ta(NMe_2)_5$ was among the very first reported early-transition-metal complexes as hydroaminoalkylation pre-catalyst under thermal conditions,[56] and has been used as Ta source in catalytic hydroaminoalkylation.[57–62] Our initial investigation was conducted using 10 mol% $Ta(NMe_2)_5$ loading and *N*-methylaniline/1-octene as the model substrate combination. Notably, there have been no previous reports for the photocatalytic hydroaminoalkylation of simple unactivated alkenes. Here, the reaction mixture was irradiated by a domestic G4 light bulb with UV filter at room temperature for 20 h (Fig. S1†). The reaction progress was monitored by ^{1}H-NMR spectroscopy and the NMR yield of hydroaminoalkylation product formation was determined by comparing the *ortho*-H integration of the product *vs.* the 1,3,5-trimethoxybenzene internal standard. Unfortunately, the use of known thermally catalytically active $Ta(NMe_2)_5$ offered no observable reactivity after irradiating for 20 h (Table 1, entry 1). Interestingly, by switching to $Ta(CH_2SiMe_3)_3Cl_2$ (**Ta1**) trace (around 4%) hydroaminoalkylation product could be observed (entry 2). Consequently, we conducted further ligand screening using **Ta1** as the Ta source.

Table 1 Metal and ligand dependence in photocatalyzed hydroaminoalkylation

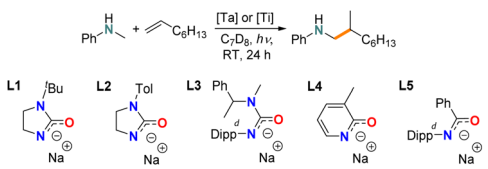

Entry	Precatalyst	Ligand	Loading (mol%)	Yield[a] (%)
1	$Ta(NMe_2)_5$	—	10	0
2	$Ta(CH_2SiMe_3)_3Cl_2$	—	10	4
3	$Ta(CH_2SiMe_3)_3Cl_2$	**L1**	10	30 (91)[b]
4	$Ta(CH_2SiMe_3)_3Cl_2$	**L1**	10	0[c]
5	$Ta(CH_2SiMe_3)_3Cl_2$	**L1**	0	0
6	—	**L1H**	10	0
7	$Ta(CH_2SiMe_3)_3Cl_2$	**L2**	10	10
8	$Ta(CH_2SiMe_3)_3Cl_2$	**L3**	10	0
9	$Ta(CH_2SiMe_3)_3Cl_2$	**L4**	10	0
10	$Ta(CH_2SiMe_3)_3Cl_2$	**L5**	10	0
11	$Ti(Bn)_4$	**L1**	10	0
12	$Ti(CH_2SiMe_3)_4$	**L1**	10	0
13	$Zr(Bn)_4$	**L1**	10	0

[a] Determined by ^{1}H NMR. [b] Yield after 72 h. [c] No light. [d] Dipp – 2,6-diisopropylphenyl.

Open Access Article. Published on 19 April 2023. Downloaded on 2/11/2026 12:40:17 AM. This article is licensed under a Creative Commons Attribution-NonCommercial 3.0 Unported Licence.

We then tested a *N*,*O*-chelated cyclic ureate ligand **L1** on **Ta1**, which offers turnover frequencies of up to 60 h^{-1} at 110 °C for thermally promoted hydroaminoalkylation.[28] A yield of 30% was achieved after 24 h irradiation, and finally reached almost quantitative yield (91%) after 3 days (entry 3). Importantly, the branched product was formed exclusively, which is aligned with thermally promoted early-transition-metal-catalyzed-hydroaminoalkylation.[18] In a control reaction, the experiment was conducted under complete exclusion of light by covering the sample with aluminum foil (**Entry 4**). Here, no conversion was observed, confirming this is a photocatalyzed process. Furthermore, by only using the substrates without the catalyst system **Ta1**/**L1** (**Entry 5**) or only using the proteo ligand (**Entry 6**) no conversion was observed, confirming that Ta is crucial to this photocatalytic transformation. With identification of the crucial role of Ta, the 1,3-*N*,*O*-chelating ligand **L1** and $-CH_2SiMe_3$ auxiliary ligands, we then tested several other 1,3-*N*,*O*-chelating ligands (**L2**–**L5**, entries 7–10) that are known to promote high catalytic activity in tantalum-catalyzed hydroaminoalkylation under thermal conditions.[27,28,63,64] Here, the acyclic ureate **L3**, pyridonate **L4** and amidate **L5** all showed no activity at all while the cyclic ureate **L2**, which changes the ^{t}Bu substituent on the non-ligating nitrogen of **L1** to 4-tolyl, shows inferior reactivity towards **L1** (10%).

To explain the difference in photocatalytic reactivities of **Ta1**/**L1**–**Ta1**/**L5**, which are all known good hydroaminoalkylation catalyst under thermal conditions, we computationally explored the differences in photo-excited states of these compounds. To interpret the influence of ligand over the photocatalytic reactivity of Ta compounds, we chose **TaL1** and **TaL4** as examples for computational analysis.

Based on TD-DFT calculations on **Ta1**/**L1**, the tris-alkyl-mono-chloro-tantalum ureate pre-catalyst has no absorption in the visible region, which matches the experimentally measured UV-Vis absorption (Fig. S6†). However, a small absorption band at around 483 nm was identified with a tantalaaziridine complex bearing **L1** ligand (Fig. S7.2†). This computational observation is close to the experimentally observed wavelength of maximum reactivity (440 nm, see ESI† for determination of wavelength dependency of reactivity). We then further computationally compared the excitation process of tantalaaziridine complexes bearing **L1** and **L4**.

In the case of **Ta**/**L1**, which has a ureate ligand on Ta, the excitation process is a ligand to metal charge transfer (LMCT) process (Fig. 1, top),[49,50] which has been demonstrated as a unique feature for early transition metal based photocatalysis.[65] With the charge transfer from the aziridine ligand to the tantalum metal center, the Ta–C bond is weakened as indicated by an increase in bond length (2.134 *vs.* 2.236 Å). However in the case of **Ta**/**L4** which has a pyridonate ligand, the excitation is not only LMCT but also has ligand to ligand charge transfer features from amido to pyridonate ligand (Fig. 1, bottom). The resultant elongation of the Ta–C bond length is also not as significant (2.148 *vs.* 2.219 Å). Furthermore, the singly occupied natural orbitals of **Ta**/**L4** delocalize across the amido and pyridonate ligands, while they are localized on the tantalum aziridine moiety on **Ta**/**L1** (Fig. S4 and S5†). This

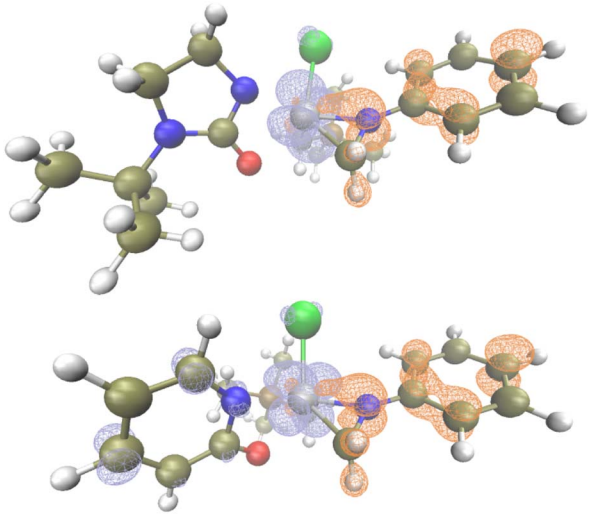

Fig. 1 Excitation analysis of TaL1 (top) and TaL2 in toluene, and electrons (blue) and holes (orange) after excitation (opt: M06L-D3/Def2SVP, TD: M06L-D3/Def2TZVPP, isovalue = 0.05).

suggests that the conjugated pyridonate ligand energetically stabilizes the charge transfer species, disfavoring Ta–C bond cleavage. Therefore the excited state has less LMCT character, meaning lower population of the partially antibonding Ta–C molecular orbital.

Finally, we tested several other homoleptic early-transition-metal-alkyl complexes that are known hydroaminoalkylation catalysts, such as $Ti(CH_2SiMe_3)_4$ and $ZrBn_4$,[22,27,66] With **L1** ligand, none of them gave observable photoreactivity (entries 11–13), suggesting the unique reactivity of the Ta complex under photonic excitation.

Substrate screening

After confirming the room temperature photocatalytic reactivity of **Ta1**/**L1** system for the hydroaminoalkylation of *N*-methylaniline and 1-octene, next a comparison to the thermally promoted reaction (>110 °C) was completed with various substrates. Specifically, we are interested in establishing the scope and functional group tolerance of this system, to determine the similarities and differences in substrate scope between the photocatalytic and thermally promoted reactions.

For the identification of the substrate scope for photocatalytic hydroaminoalkylation using **Ta1**/**L1** similar NMR-screening techniques were applied (Scheme 2). To maximize yields, the reaction time was increased to 72 h.

Similar to the reaction of 1-octene, other unactivated terminal alkenes like 4-phenyl-1-butene gave a high yield (88%). By increasing the steric bulk next to the alkene functionality, while maintaining an alkyl substituted alkene *e.g.* vinylcyclohexane, the reactivity drops significantly (45%). However, with addition of just one methylene unit in the carbon chain, even larger substituents like -OTBDMS are tolerated very well (68%).

Furthermore, we tested internal alkenes, which are generally known to be very challenging substrates in early transition

© 2023 The Author(s). Published by the Royal Society of Chemistry

Open Access Article. Published on 19 April 2023. Downloaded on 2/11/2026 12:40:17 AM.
This article is licensed under a Creative Commons Attribution-NonCommercial 3.0 Unported Licence.

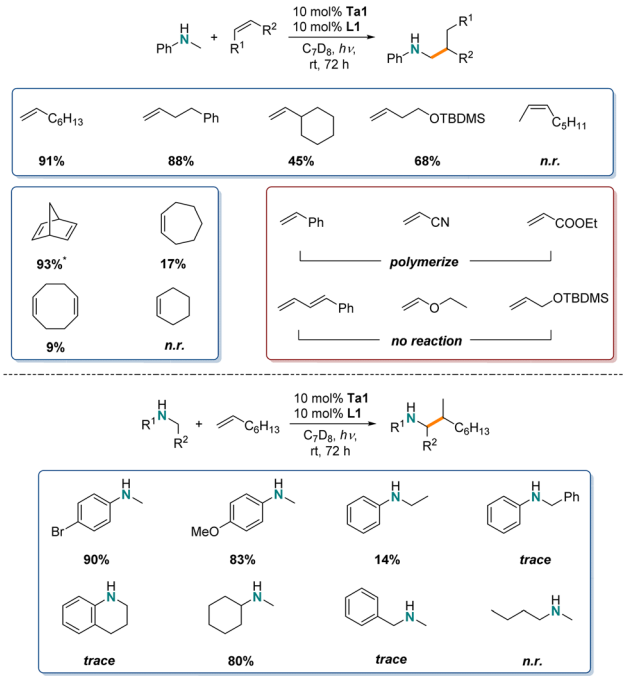

Scheme 2 Substrate scope of **Ta1** and **L1** for photocatalytic hydroaminoalkylation of various amines and alkenes. Yields were determined by integration in ^{1}H-NMR *vs.* internal standard (*: mixture of both mono- and bis-alkylation, consumption of amine substrate *vs.* internal standard is reported), *trace* means detectable by ^{1}H-NMR but below quantification criteria (2%), *n.r.* means no detected product by both ^{1}H-NMR and GC-MS.

metal catalyzed-hydroaminoalkylation.[18,19] Here, acyclic internal 2-octene showed no reactivity, while strained cyclic alkenes like norbornadiene showed near quantitative substrate consumption (93%) (producing mixtures of both mono- and bis-alkylated products as well as ring-opening polymerized product). Less strained cyclic alkene like cycloheptene (17%), 1,5-cyclooctadiene (9%) and cyclohexene (n.r.) showed poor reactivity, as has been observed under thermal conditions.

These first photocatalytic results show reduced catalytic activity in comparison to the thermal variant of tantalum catalyzed hydroaminoalkylation as longer reaction times are required to reach comparable yields,[28] but they do show that unactivated alkenes can be used in photocatalyzed hydroaminoalkylation. In our case, unlike LTM photocatalysts which favour Michael acceptors as activated alkene substrates, the **Ta1**/**L1** system did not catalyze hydroaminoalkylation of styrene or α,β-unsaturated alkenes like acrylonitrile or ethyl acrylate but instead caused polymerization, as observed by the formation of either brittle solids inside the NMR tube or broad signals in the ^{1}H-NMR spectra. Additionally, conjugated dienes, vinyl ethers or allyl ethers were unreactive under standard conditions. This photocatalytic hydroaminoalkylation (α-C–H alkylation of amines) using a Ta based photosensitizer offers complementary substrate scope to the work using established LTM based photoredox catalysts.

For the amine scope, both electron withdrawing (–Br, 90%) and electron donating (-OMe, 83%) *para*-substituents for *N*-methylanilines showed high reactivity. Here, especially the halide substituents are of interest, because such aryl halides can then be used in further cross-coupling reactions with late-transition metal catalysts.[67,68] Varying the *N*-alkyl substituent led to decreased reactivity: *N*-ethyl- (14%), *N*-benzylaniline (trace) and tetrahydroquinoline (trace). Interestingly, by switching to dialkylated amines, the yields for *N*-methylcyclohexylamine are similar to those of the *N*-methylaniline derivates (80%). However, sterically less demanding substituents like *N*-methylbenzylamine (trace) and *N*-methyl-*n*-butylamine (n.r.) led to a drastic decrease in reactivity. This suggests that secondary amines with bulky groups are preferred for this photocatalytic reaction. Tertiary amines were also unreactive in these conditions (*vide infra*).

Finally, we were interested in the intramolecular hydroaminoalkylation of aminoalkenes leading to ring-closure. While there are examples of group 4 metal catalysts for this transformation,[62,66,69,70] to date, tantalum has not been reported for this reaction. Here, we show (Scheme 3) that intramolecular hydroaminoalkylation of aminoalkene furnishes the cyclopentylamine derivative using **Ta1**/**L1**.

Mechanistic probes

α-Aminoalkyl radicals are involved in LTM catalyzed photoredox hydroaminoalkylation,[2] and tertiary amines, such as *N*,*N*-dimethylaniline, are preferred substrates due the increased stability of tertiary amine radical.[71] In contrast to that, early-transition-metal-catalyzed thermal hydroaminoalkylation requires the use of secondary or primary amines as substrates to access the requisite metallaaziridine reactive intermediates.[17,18,72,73]

For our photocatalytic process at room temperature, *N*,*N*-dimethylaniline gave no conversion, suggesting that tantalum amido intermediates are involved in the mechanistic cycle (Scheme 4a). To test the involvement of radicals, the irradiation of *N*-(cyclopropylmethyl)toluidine with 20 mol% tantalum ureate complex for 20 h, in the absence of alkene substrate showed alkene signals forming in the ^{1}H NMR spectrum, consistent with ring-opening of the cyclopropyl unit (Scheme 4b). However, a similar experiment with only the alkene substrate 2-cyclopropylpropene (Scheme 4c) resulted in no observable ring-opening. While the addition of the same substrate to *N*-methylaniline under photocatalytic conditions resulted in one single product (identified by GC-MS, ESI 8.2†). NMR spectroscopy showed that the cyclopropyl group was untouched. Based on these mechanism probes, formation of metal-amido based radicals as a key intermediate prior to the C–C bond forming step is proposed to be involved.

Finally, in a control reaction, TEMPO was explored as an alternative radical source to promote the reaction of *N*-

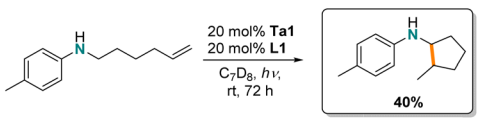

Scheme 3 Photocatalytic intramolecular hydroamino-alkylation of aminoalkenes.

Open Access Article. Published on 19 April 2023. Downloaded on 2/11/2026 12:40:17 AM.
This article is licensed under a Creative Commons Attribution-NonCommercial 3.0 Unported Licence.

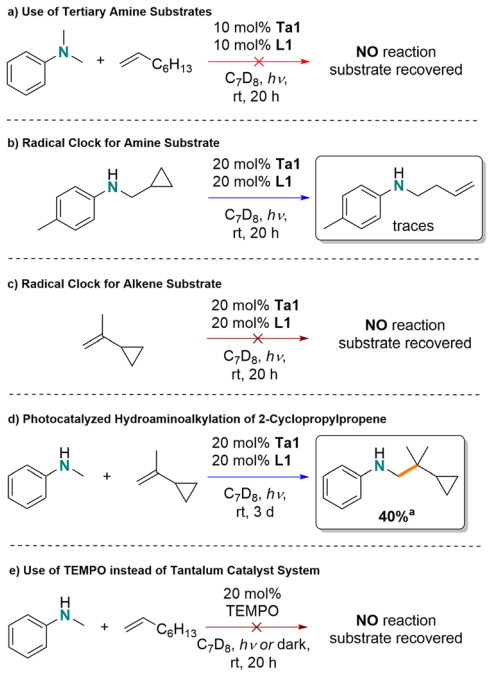

Scheme 4 Mechanism probes evaluating the photocatalyzed hydroaminoalkylation by Ta1/L1; [a]NMR yield.

methylaniline and 1-octene (Scheme 4e). Here, no conversion was observed either in the dark or under light irradiation, suggesting that the reaction is not just initiated by radicals. Additionally, irradiating a reaction containing both **Ta1**/**L1** and TEMPO led to no product formation, which may be due to the formation of an inactive Ta–TEMPO complex.

Based on these control experiments and our computational observations, we postulate the formation of a metallaaziridine species that undergoes a metal–carbon homolytic cleavage (see Scheme 6, **B**) as the key species that adds to coordinated alkene for photocatalytic hydroaminoalkylation. We demonstrated in the ligand screening (Table 1) that some of the *N*,*O*-chelating ligands with conjugated moieties such as pyridonate **L4** or the phenyl substituted ureate **L2** exhibit no or inferior reactivity compared to the alkyl substituted cyclic ureate **L1**. Consequently, we hypothesized that ligand aromatic moieties may

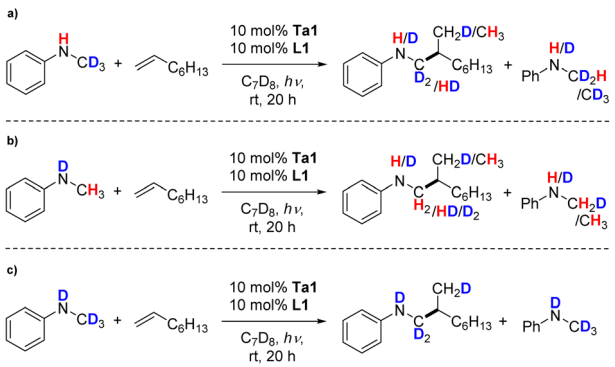

Scheme 5 Kinetic isotope labelling experiments of the hydroaminoalkylation of (a) *C*-, (b) *N*- and (c) *C*,*N*-deuterated *N*-methylaniline with 1-octene using Ta1/L1.

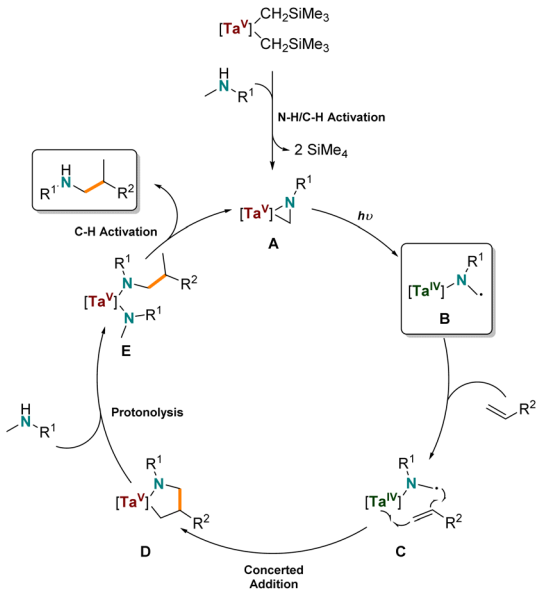

Scheme 6 Proposed mechanism for the photocatalytic tantalum-catalyzed intermolecular hydroaminoalkylation of alkenes.

stabilize such photogenerated radicals and inhibit radical addition to the alkene substrate.

After these initial experiments testing our mechanistic hypothesis, we performed isotope labeling experiments for a direct comparison to the thermal hydroaminoalkylation process. For this, we used again the model reaction of 1-octene with partially or fully deuterated versions of *N*-methylaniline in crucial N–H and/or $-CH_3$ positions using our photocatalytic conditions. Here, for $PhNDCH_3$ and $PhNHCD_3$ proton/deuteron scrambling in the substrates as well as in the products was observed (Scheme 5a and b). This indicates reversible formation of a tantalaaziridine key intermediate, which is the same catalytically active species for thermally promoted group 5 metal catalyzed hydroaminoalkylations.[18,59,72–74] Finally, no *ortho*-deuteration on the phenyl ring of the hydroaminoalkylation product was found. This behavior is different from the thermal version of hydroaminoalkylation catalyzed by cyclic ureate complexes of tantalum and other group 5 complexes,[28] and consequently indicates that a side reaction of reversible aromatic C–H bond activation does not occur here.

An evaluation of kinetic isotope effects (KIE) (Fig. S2†) found that small KIEs were observed for both k_{NH}/k_{ND} and k_{CH_3}/k_{CD_3} (values were found to be 1.5 and 1.9 respectively), which is different from the thermally promoted reaction, where only the N–H bond displayed a KIE > 1.[28] Additionally, long induction periods were observed. Therefore, neither C–H nor N–H activation is invoked as being involved in the turnover limiting step.

Based on these investigations, we propose the following reaction mechanism (Scheme 6) that is similar to the mechanism of the thermal hydroaminoalkylation reaction by early transition metals. First, the organometallic tantalum pre-catalyst undergoes protonolysis with a secondary amine to generate the catalytically active tantalum(v) aziridine (**A**) *via* N–H/C–H activation and elimination of tetramethylsilane, as

© 2023 The Author(s). Published by the Royal Society of Chemistry

Open Access Article. Published on 19 April 2023. Downloaded on 2/11/2026 12:40:17 AM. This article is licensed under a Creative Commons Attribution-NonCommercial 3.0 Unported Licence.

observed by ^{1}H NMR spectroscopy. Due to the fact that alkene based radicals are ruled out (see Scheme 4c and d) but tantalum amido radicals are likely to be involved we propose a tantalum(IV) amido diradical (**B**) is formed by photolytically induced homolytic cleavage of the Ta–C bond of **A**. This can undergo addition to coordinated alkene (**C**) to give the tantalum(V) azacyclopentane (**D**). **D** is a common intermediate to the thermally promoted hydroaminoalkylation mechanism, and rationalizes the same branched regioselectivity of thermally promoted Ta-catalyzed hydroaminoalkylation. Finally, and in accordance to the labeling experiments, **D** reacts *via* protonolysis of the Ta–C bond of the metallacycle, resulting in the formation of a new bisamido intermediate (**E**). After another C–H activation step, the product is released from the metal center and the starting catalytically active tantalaaziridine (**A**) is formed again.

Conclusions

In summary, here we report the first example of photocatalyzed hydroaminoalkylation using an early-transition-metal catalyst. The system of **Ta1** and **L1** undergoes simple hydroaminoalkylation reactions using a G4 tungsten halogen light bulb at room temperature instead of temperatures at 110 °C or higher, which are commonly used for early-transition-metal-catalyzed hydroaminoalkylation. We demonstrated the reactivity of this catalyst with a series of unprotected amines and unactivated alkene substrates, showing that the reaction can proceed with even the most challenging unactivated substrates that are unknown for established LTM photoredox catalyzed hydroaminoalkylation. Furthermore, we showed the first example of cyclization of an aminoalkene using a tantalum-based catalyst. Using reaction kinetics, and mechanistic probe experiments we propose a mechanism for tantalum catalyzed radical reactions for hydroaminoalkylation and using computational approaches we rationalize the observed ligand dependence of this reactivity. We propose that LMCT resulting in homolytic Ta–C bond cleavage is key to this light-promoted variant, while the other steps are comparable to the known mechanistic cycle for early transition metal catalyzed hydroaminoalkylation. We propose that these insights can be leveraged to realize improved catalyst development featuring inexpensive and low-toxicity early-transition-metal catalysts for increased photocatalytic reactivity in hydroaminoalkylation and other challenging C–E bond forming reactions at low temperatures.

Data availability

ESI† is available; including experimental details, computational, photophysical and spectroscopic characterization data.

Author contributions

H. H. conceived the project; H. H. and M. M. conducted experiments in consultation with L. L. S.; H. H. conducted computations; H. H. and M. M. prepared the draft of the manuscript; L. L. S. contributed with an advisory role in the project and manuscript.

Conflicts of interest

The authors declare no conflict of interest.

Acknowledgements

Funding from NSERC and the Feodor Lynen Postdoctoral Fellowship of the Humboldt-Foundation: Germany, Funder ID: 100005156 to M. M. is gratefully acknowledged. This work has been supported in part by the Canada Research Chairs program.

Notes and references

1 R. C. DiPucchio, K. E. Lenzen, P. Daneshmand, M. B. Ezhova and L. L. Schafer, *J. Am. Chem. Soc.*, 2021, **143**, 11243–11250.
2 A. Trowbridge, S. M. Walton and M. J. Gaunt, *Chem. Rev.*, 2020, **120**, 2613–2692.
3 Z. Dong, Z. Ren, S. J. Thompson, Y. Xu and G. Dong, *Chem. Rev.*, 2017, **117**, 9333–9403.
4 S. Zhu and D. Wang, *Adv. Energy Mater.*, 2017, **7**, 1700841.
5 J. J. Murphy, D. Bastida, S. Paria, M. Fagnoni and P. Melchiorre, *Nature*, 2016, **532**, 218–222.
6 R. A. Aycock, C. J. Pratt and N. T. Jui, *ACS Catal.*, 2018, **8**, 9115–9119.
7 Y. Miyake, Y. Ashida, K. Nakajima and Y. Nishibayashi, *Chem. Commun.*, 2012, **48**, 6966–6968.
8 L. Ruiz Espelt, I. S. McPherson, E. M. Wiensch and T. P. Yoon, *J. Am. Chem. Soc.*, 2015, **137**, 2452–2455.
9 S.-X. Lin, G.-J. Sun and Q. Kang, *Chem. Commun.*, 2017, **53**, 7665–7668.
10 X. Shen, Y. Li, Z. Wen, S. Cao, X. Hou and L. Gong, *Chem. Sci.*, 2018, **9**, 4562–4568.
11 K. Miyazawa, T. Koike and M. Akita, *Adv. Synth. Catal.*, 2014, **356**, 2749–2755.
12 B. M. Hockin, C. Li, N. Robertson and E. Zysman-Colman, *Catal. Sci. Technol.*, 2019, **9**, 889–915.
13 C. B. Larsen and O. S. Wenger, *Chem.–Eur. J.*, 2018, **24**, 2039–2058.
14 S. Parisien-Collette, A. C. Hernandez-Perez and S. K. Collins, *Org. Lett.*, 2016, **18**, 4994–4997.
15 J.-R. Jiménez, B. Doistau, C. Besnard and C. Piguet, *Chem. Commun.*, 2018, **54**, 13228–13231.
16 T. P. Nicholls, G. E. Constable, J. C. Robertson, M. G. Gardiner and A. C. Bissember, *ACS Catal.*, 2016, **6**, 451–457.
17 M. Manßen and L. L. Schafer, *Trends Chem.*, 2021, **3**, 428–429.
18 M. Manßen and L. L. Schafer, *Chem. Soc. Rev.*, 2020, **49**, 6947–6994.
19 P. M. Edwards and L. L. Schafer, *Chem. Commun.*, 2018, **54**, 12543–12560.
20 L. L. Schafer, M. Manßen, P. M. Edwards, E. K. J. Lui, S. E. Griffin and C. R. Dunbar, in *Advances in Organometallic Chemistry*, Elsevier, 2020, vol. 74, pp. 405–468.
21 M. G. Clerici and F. Maspero, *Synthesis*, 2002, **1980**, 305–306.

© 2023 The Author(s). Published by the Royal Society of Chemistry

Open Access Article. Published on 19 April 2023. Downloaded on 2/11/2026 12:40:17 AM. This article is licensed under a Creative Commons Attribution-NonCommercial 3.0 Unported Licence.

22 T. Kaper, D. Geik, F. Fornfeist, M. Schmidtmann and S. Doye, *Chem.–Eur. J.*, 2022, **28**, e202103931.
23 M. Rosien, I. Töben, M. Schmidtmann, R. Beckhaus and S. Doye, *Chem.–Eur. J.*, 2020, **26**, 2138–2142.
24 J. Dörfler, T. Preuß, A. Schischko, M. Schmidtmann and S. Doye, *Angew. Chem., Int. Ed.*, 2014, **53**, 7918–7922.
25 J. Bielefeld and S. Doye, *Angew. Chem., Int. Ed.*, 2020, **59**, 6138–6143.
26 M. Manßen, D. Deng, C. H. M. Zheng, R. C. DiPucchio, D. Chen and L. L. Schafer, *ACS Catal.*, 2021, **11**, 4550–4560.
27 R. C. DiPucchio, S.-C. Roşca and L. L. Schafer, *Angew. Chem., Int. Ed.*, 2018, **57**, 3469–3472.
28 P. Daneshmand, S.-C. Roşca, R. Dalhoff, K. Yin, R. C. DiPucchio, R. A. Ivanovich, D. E. Polat, A. M. Beauchemin and L. L. Schafer, *J. Am. Chem. Soc.*, 2020, **142**, 15740–15750.
29 J. Bielefeld and S. Doye, *Angew. Chem., Int. Ed.*, 2017, **56**, 15155–15158.
30 E. N. Bahena, S. E. Griffin and L. L. Schafer, *J. Am. Chem. Soc.*, 2020, **142**, 20566–20571.
31 M. Manßen, N. Lauterbach, J. Dörfler, M. Schmidtmann, W. Saak, S. Doye and R. Beckhaus, *Angew. Chem., Int. Ed.*, 2015, **54**, 4383–4387.
32 P. Garcia, Y. Y. Lau, M. R. Perry and L. L. Schafer, *Angew. Chem., Int. Ed.*, 2013, **52**, 9144–9148.
33 A. E. Nako, J. Oyamada, M. Nishiura and Z. Hou, *Chem. Sci.*, 2016, **7**, 6429–6434.
34 F. Liu, G. Luo, Z. Hou and Y. Luo, *Organometallics*, 2017, **36**, 1557–1565.
35 D. Geik, M. Rosien, J. Bielefeld, M. Schmidtmann and S. Doye, *Angew. Chem., Int. Ed.*, 2021, **60**, 9936–9940.
36 G. J. Choi, Q. Zhu, D. C. Miller, C. J. Gu and R. R. Knowles, *Nature*, 2016, **539**, 268–271.
37 A. J. Musacchio, B. C. Lainhart, X. Zhang, S. G. Naguib, T. C. Sherwood and R. R. Knowles, *Science*, 2017, **355**, 727–730.
38 Y. Miyake, K. Nakajima and Y. Nishibayashi, *J. Am. Chem. Soc.*, 2012, **134**, 3338–3341.
39 X. Dai, D. Cheng, B. Guan, W. Mao, X. Xu and X. Li, *J. Org. Chem.*, 2014, **79**, 7212–7219.
40 S. M. Thullen and T. Rovis, *J. Am. Chem. Soc.*, 2017, **139**, 15504–15508.
41 J. Ye, I. Kalvet, F. Schoenebeck and T. Rovis, *Nat. Chem.*, 2018, **10**, 1037–1041.
42 J. B. McManus, N. P. R. Onuska and D. A. Nicewicz, *J. Am. Chem. Soc.*, 2018, **140**, 9056–9060.
43 X. Ju, D. Li, W. Li, W. Yu and F. Bian, *Adv. Synth. Catal.*, 2012, **354**, 3561–3567.
44 S. Zhu, A. Das, L. Bui, H. Zhou, D. P. Curran and M. Rueping, *J. Am. Chem. Soc.*, 2013, **135**, 1823–1829.
45 X. Dai, R. Mao, B. Guan, X. Xu and X. Li, *RSC Adv.*, 2015, **5**, 55290–55294.
46 H. E. Askey, J. D. Grayson, J. D. Tibbetts, J. C. Turner-Dore, J. M. Holmes, G. Kociok-Kohn, G. L. Wrigley and A. J. Cresswell, *J. Am. Chem. Soc.*, 2021, **143**, 15936–15945.
47 R. Gazzi, F. Perazzolo, S. Sostero, A. Ferrari and O. Traverso, *J. Organomet. Chem.*, 2005, **690**, 2071–2077.
48 E. Samuel, P. Maillard and C. Giannotti, *J. Organomet. Chem.*, 1977, **142**, 289–298.
49 H. B. Abrahamson, K. L. Brandenburg, B. Lucero, M. E. Martin and E. Dennis, *Organometallics*, 1984, **3**, 1379–1386.
50 H. B. Abrahamson and M. E. Martin, *J. Organomet. Chem.*, 1982, **238**, C58–C62.
51 L. R. Chamberlain and I. P. Rothwell, *J. Chem. Soc., Dalton Trans.*, 1987, 163–167.
52 Y. Zhang, J. L. Petersen and C. Milsmann, *J. Am. Chem. Soc.*, 2016, **138**, 13115–13118.
53 Y. Zhang, D. C. Leary, A. M. Belldina, J. L. Petersen and C. Milsmann, *Inorg. Chem.*, 2020, **59**, 14716–14730.
54 Y. Zhang, J. L. Petersen and C. Milsmann, *Organometallics*, 2018, **37**, 4488–4499.
55 Y. Zhang, T. S. Lee, J. L. Petersen and C. Milsmann, *J. Am. Chem. Soc.*, 2018, **140**, 5934–5947.
56 S. B. Herzon and J. F. Hartwig, *J. Am. Chem. Soc.*, 2007, **129**, 6690–6691.
57 P. Eisenberger, R. O. Ayinla, J. M. P. Lauzon and L. L. Schafer, *Angew. Chem., Int. Ed.*, 2009, **48**, 8361–8365.
58 A. L. Reznichenko, T. J. Emge, S. Audörsch, E. G. Klauber, K. C. Hultzsch and B. Schmidt, *Organometallics*, 2011, **30**, 921–924.
59 J. M. Lauzon, P. Eisenberger, S.-C. Roşca and L. L. Schafer, *ACS Catal.*, 2017, **7**, 5921–5931.
60 J. Dörfler and S. Doye, *Eur. J. Org. Chem.*, 2014, **2014**, 2790–2797.
61 G. Zi, F. Zhang and H. Song, *Chem. Commun.*, 2010, **46**, 6296–6298.
62 P. Garcia, P. R. Payne, E. Chong, R. L. Webster, B. J. Barron, A. C. Behrle, J. A. R. Schmidt and L. L. Schafer, *Tetrahedron*, 2013, **69**, 5737–5743.
63 R. C. DiPucchio, S.-C. Rosca, G. Athavan and L. L. Schafer, *ChemCatChem*, 2019, **11**, 3871–3876.
64 E. Chong, J. W. Brandt and L. L. Schafer, *J. Am. Chem. Soc.*, 2014, **136**, 10898–10901.
65 Y. Zhang, T. S. Lee, J. M. Favale, D. C. Leary, J. L. Petersen, G. D. Scholes, F. N. Castellano and C. Milsmann, *Nat. Chem.*, 2020, **12**, 345–352.
66 I. Prochnow, R. Kubiak, O. N. Frey, R. Beckhaus and S. Doye, *ChemCatChem*, 2009, **1**, 162–172.
67 Z. Zhang, J.-D. Hamel and L. L. Schafer, *Chem.–Eur. J.*, 2013, **19**, 8751–8754.
68 M. Weers, L. H. Lühning, V. Lührs, C. Brahms and S. Doye, *Chem.–Eur. J.*, 2017, **23**, 1237–1240.
69 J. A. Bexrud, P. Eisenberger, D. C. Leitch, P. R. Payne and L. L. Schafer, *J. Am. Chem. Soc.*, 2009, **131**, 2116–2118.
70 J. Dörfler, B. Bytyqi, S. Hüller, N. M. Mann, C. Brahms, M. Schmidtmann and S. Doye, *Adv. Synth. Catal.*, 2015, **357**, 2265–2276.
71 J. Hioe, D. Šakić, V. Vrček and H. Zipse, *Org. Biomol. Chem.*, 2015, **13**, 157–169.
72 I. Prochnow, P. Zark, T. Müller and S. Doye, *Angew. Chem., Int. Ed.*, 2011, **50**, 6401–6405.
73 D. J. Gilmour, J. M. P. Lauzon, E. Clot and L. L. Schafer, *Organometallics*, 2018, **37**, 4387–4394.
74 A. L. Reznichenko and K. C. Hultzsch, *J. Am. Chem. Soc.*, 2012, **134**, 3300–3311.

© 2023 The Author(s). Published by the Royal Society of Chemistry